
A Fast Training-Free Compression Framework for Vision Transformers

Jung Hwan Heo¹ Arash Fayyazi¹ Mahdi Nazemi¹ Massoud Pedram¹

Abstract

Token pruning has emerged as an effective solution to speed up the inference of large Transformer models. However, prior work on accelerating Vision Transformer (ViT) models requires training from scratch or fine-tuning with additional parameters, which prevents a simple plug-and-play. To avoid high training costs during the deployment stage, we present a fast *training-free* compression framework enabled by (i) a dense feature extractor in the initial layers; (ii) a sharpness-minimized model which is more compressible; and (iii) a local-global token merger that can exploit spatial relationships at various contexts. We applied our framework to various ViT and DeiT models and achieved up to $2\times$ reduction in FLOPS and $1.8\times$ speedup in inference throughput with $<1\%$ accuracy loss, while saving *two orders of magnitude shorter training times* than existing approaches.²

1. Introduction

The emergence of Transformers (Vaswani et al., 2017) as a general-purpose backbone architecture has resulted in great progress in a wide range of applications, ranging from natural language processing (Devlin et al., 2019), speech recognition (Tian et al., 2020), to computer vision (Dosovitskiy et al., 2020). Compared to Convolutional Neural Networks (CNNs), Vision Transformers (ViTs) have a minimal inductive bias which benefits from large-scale pretraining. For example, state-of-the-art self-supervised pretraining techniques such as MAE obtains up to 90.94% top-1 accuracy on ImageNet-1k (Wortsman et al., 2022). For supervised learning scenarios, DeiT models receive extra supervision through distillation (Touvron et al., 2021), and Swin transformers design vision-specific inductive bias that exploits locality (Liu et al., 2021a) to further boost performance.

¹Department of Electrical and Computer Engineering, University of Southern California, Los Angeles, United States. Correspondence to: Jung Hwan Heo <jhjohnheo@gmail.com>.

²Code will be available at <https://github.com/johnheo/fast-compress-vit>

However, efficient deployment of ViTs remains a challenge due to the large model size and high inference latency (Rao et al., 2021). In addition to pruning or quantization techniques (Zhang et al., 2022; Shen et al., 2020) that generally apply to both convolution-based and transformer-based models, recent work takes advantage of the input-agnostic nature that is unique to ViT. Since the inputs in ViT are represented as non-overlapping tokens, less informative tokens can be pruned at runtime to accelerate inference throughput (Rao et al., 2021; Yin et al., 2022; Liang et al., 2022).

A major line of work has focused on identifying and pruning task-irrelevant tokens with various importance heuristics such as token embeddings (Yin et al., 2022), attention scores (Liang et al., 2022), and lightweight neural network predictors (Rao et al., 2021). Recently, a newly proposed token *merging* scheme enabled a *training-free* approach to token reduction for the first time (Bolya et al., 2022).

While prior works can effectively reduce inference time, it is still difficult to use these techniques in practice for various reasons. Previous approaches train from scratch (Liang et al., 2022), fine-tune with extra parameters (Rao et al., 2021), and optimize with additional loss functions that increase the wall-clock training time (Yin et al., 2022). Such complexities introduce extra computational budgets and engineering efforts that prevent users from easily adapting the techniques to their own use cases. Although the token merging scheme can avoid this by using the training-free option (Bolya et al., 2022), it can incur nontrivial accuracy loss which ultimately necessitates training from scratch to achieve competitive performance.

To resolve the aforementioned limitations, we present a fast compression framework for ViTs which increases the competitive performance of the training-free paradigm. We fully embrace token merging as an effective building block for the training-free compression pipeline and propose additional techniques to close the performance gap.

Our contributions can be summarized as follows.

- We present a fast training-free token reduction framework for ViTs, which is orders of magnitude faster than prior work. To retain accuracy, our framework employs a series of simple yet effective techniques: (i) dense feature extractor inspired by the token unifor-

mity characteristic (Section 3.1); model pretrained with sharpness-aware minimization, which helps tolerate accuracy degradation (Section 2.3); (iii) spatially-aware token merger, which can better exploit redundancies at both local and global contexts (Section 3.3).

- We extensively test our framework by applying it to both ViT and DeiT models of various sizes on ImageNet-1k. With no more than 1% drop in accuracy, our framework reduces 40% of the original FLOP count and achieves 1.6x throughput speedup on NVIDIA A6000 GPU (Figure 5).
- Lastly, we conduct a qualitative analysis of the spatially-aware token merger and show its effectiveness in merging spatially proximate tokens (Section 4.6).

2. Preliminaries

2.1. Efficient Transformers

Various research has been done to reduce the high computational cost of neural networks and enable efficient deployment to resource-constrained scenarios. At the algorithmic level, methods such as model quantization (Shen et al., 2020; Kim et al., 2021; Xiao et al., 2022), model pruning (Han et al., 2015; Voita et al., 2019; Kurtic et al., 2022), and knowledge distillation (Hinton et al., 2015; Beyer et al., 2022) have gained popularity.

Orthogonal to conventional weight pruning, another thread of work (Yin et al., 2022; Rao et al., 2021; Liang et al., 2022) has shown that transformers can be dynamically pruned at inference time. In this paper, we focus on such methods for adaptive inference which is conditioned on the input image.

2.2. Token Reduction Techniques

Token Dropping. Token reduction techniques can effectively accelerate inference. To discard redundant tokens, DynamicViT (Rao et al., 2021) trains a token importance predictor using the Gumbel-Softmax distribution. A-ViT (Yin et al., 2022) learns token importance by introducing a loss function that penalizes unpruned tokens. E-ViT (Liang et al., 2022) uses attention scores from the class token as the importance heuristic. Although these methods are effective post-deployment, they require costly retraining from scratch or finetuning from a model checkpoint, whereas our work avoids the training overheads completely (Table 1).

In addition, a majority of pruning works are dynamic, where each input example within a batch has a different number of tokens. This results in a practical hardware limitation in that batch matrix multiplications do not support dynamic sequence lengths; i.e., simply using a binary mask to emulate pruning fails to achieve wall-clock speedup (Chen et al., 2021).

Table 1. Comparison of different token reduction techniques.

	Pretrain	Finetune	Extra Params	Training-free
DynamicViT	✗	✓	✓	✗
A-ViT	✗	✓	✗	✗
E-ViT	✓	✓	✗	✗
ToMe	✓	✗	✗	✓ [†]
Ours	✗	✗	✗	✓

† susceptible to accuracy degradation.

Token Merging. Another approach for adaptive inference is token merging, combining tokens instead of pruning them. (Kong et al., 2022) proposes to fuse the to-be-pruned tokens into a single token. TokenLearner uses MLP projections (Ryoo et al., 2021) to decrease the number of tokens. Token pooling is presented as a downsampling method via merging in (Marin et al., 2021); however, its iterative kmeans-based method is slow and is not compatible with off-the-shelf models. ToMe (Bolya et al., 2022), which has been recently introduced as a token merging module utilizing a bipartite graph matching algorithm, achieves comparable accuracy to its token pruning counterparts. However, it does not use any spatial information and its accuracy loss in the high compression regime is noticeable.

2.3. Sharpness Aware Minimization

By analyzing the loss geometry, (Chen et al., 2022) has found that ViTs converge at incredibly sharp local minima, i.e., their biggest primary curvatures are almost an order of magnitude larger than that of CNNs such as ResNet. Hence, the authors apply a sharpness-aware minimizer (SAM) (Foret et al., 2021) that explicitly smooths the loss surface during training. The resulting ViT models have smoother loss landscapes and enjoy significantly improved generalization across supervised, adversarial, contrastive, and transfer learning applications. By extension, we found that having a flatter loss basin is more robust to post-training compression tasks.

2.4. Training-Free Model Compression

Post-training compression techniques have been extensively studied in quantization. Post-training quantization (PTQ) has become a popular choice in practice thanks to the ease of deployment without training, and minimal engineering effort needed for hyperparameter tuning (Kwon et al., 2022).

For ViTs, most used models in classification tasks are small (or tiny) variants in the ViT and DeiT model families. Indeed, prior token reduction techniques also experiment on small models due to the high training cost of larger models. When multiplying the training cost and the hyperparameter tuning cost, the total computing budget can be unaffordable for many researchers and practitioners (Steiner et al., 2021).

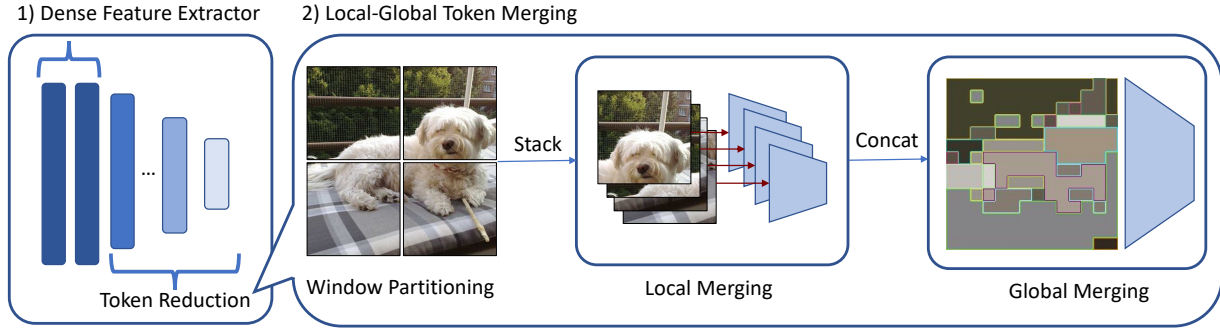


Figure 1. **Inference Pipeline.** 1) Dense Feature Extractor (DFE) delays the token merging modules to later blocks to avoid error amplification. 2) Local-Global Token Merging (LGTM) applies spatial augmentation by locally restricting the merging window.

Motivated by the fact that the highest-performing models are too expensive to compress, we propose a training-free pipeline for compressing large ViTs. We take the method’s speed as an equally-important figure of merit as the final model performance and constrain our solution to be training-free (Table 1). Our work addresses the following question: How do we compress ViTs without expensive training to realize high-accuracy inference models?

3. Training-Free Compression Framework

Overall Compression Pipeline. Figure 1 provides an overview of our proposed framework, which consists of two main stages: 1) a dense feature extractor (DFE) that does not merge in the initial layers; 2) a local-global token merging module that locally merges tokens for early layers after DFE and transitions to global merging for the rest of the network. Our findings that pertain to sharpness-aware optimizers are omitted in the figure for clarity, as it is a model selection process that precedes the inference stage.

3.1. Dense Feature Extractor (DFE)

It is common wisdom that the initial layers of a neural network act as a feature extractor (Mundhenk et al., 2019). For vision tasks, this is prominently observed in CNNs that extract low-level features in the initial layers and progressively add higher-level features towards later layers. Motivated by this, we propose a simple feature extraction technique in ViTs to improve token merging.

ToMe (Bolya et al., 2022) employs a strategy to progressively shrink the number of tokens in every transformer block to avoid sharp changes that can cause information loss. However, we find that in the context of token reduction, omitting the token merging modules for the first few layers can surprisingly boost performance up to 0.5% (Table 8), even though the tokens need to be reduced more aggressively later layers to achieve a target FLOP count. Yet, DFE has its shortcomings in high compression rates (2x FLOP reduction). A significant amount of noise is introduced from

merging tokens too quickly, and high-quality features from the dense extractor cannot overcome this noise.

To better understand this phenomenon, we measure the similarity scores between tokens for each layer of the network using the following equation:

$$\text{CosSim} = \frac{1}{n(n-1)} \sum_{i \neq j} \frac{h_i^T h_j}{\|h_i\|_2 \|h_j\|_2}$$

Here, h is a sequence of n tokens $h = [h_{cls}, h_1, \dots, h_n]$. A higher CosSim score indicates that the tokens in that layer have similar embeddings. The progression of this is plotted in Figure 2 where $X_{preAttn}$ is before, X_{Attn} is during, and $X_{postAttn}$ is after the attention block.

Interestingly, we find that for the first two layers of DeiT-S, the tokens are *diversifying*. Subsequently, they converge and have progressively similar representations. We speculate that merging tokens that are in the process of diversifying

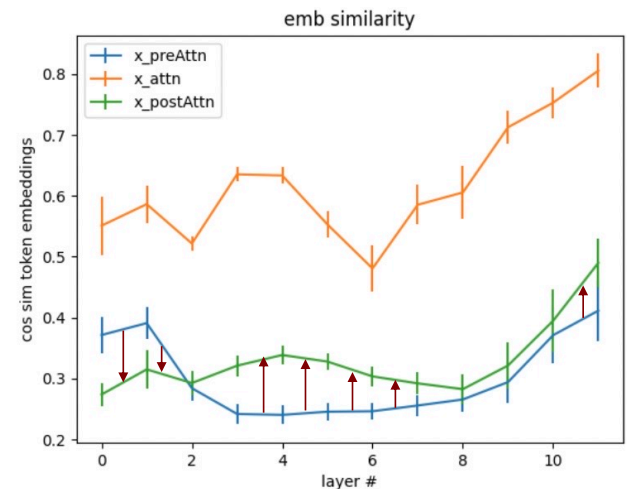


Figure 2. Divergence and convergence trends of token embeddings across different layers on DeiT-S.

is challenging, as the tokens are still learning the correct representations. Once the embeddings stabilize, it is easier to identify similar tokens to merge. Hence, we skip merging for the first one-sixth of the network depth. We provide further ablations in Table 6.

3.2. Compressibility of SAM Models

Previous work has explored the relationship between compression and generalization, where model compression can act as a regularizer for finding more simpler solutions that generalize well, and vice-versa. Thus, generalizability as a proxy training target (Foret et al., 2021; Chen et al., 2022) can lead to compressibility as a desirable side-effect.

Model Selection. Given this insight, it is possible to choose more compression-friendly models from the beginning. In NLP tasks, (Na et al., 2022) shows that a BERT model trained with a SAM optimizer, compared to Adam (Kingma & Ba, 2014), is more robust to various compression methods such as iterative pruning, dynamic quantization, and post-training quantization.

By extension to image classification tasks, we observe the compressibility of ViTs for our dynamic inference scheme. We quantitatively validate the advantage of SAM (Table 2) by tracking the dominant Hessian eigenvalue λ_{max} of the trained model, which measures the worst-case loss curvature. With the vanilla ToMe module (Bolya et al., 2022), ViT-B trained with SAM can minimize the increase in sharpness from $9.9\times$ to $1.6\times$. With DFE, it can boost the accuracy by 1.1% achieve *lossless* compression.

Table 2. Classification accuracy and the sharpness of local minima λ_{max} of the ViT-B/16 model. \curvearrowright indicates skip value.

Approach	Accuracy (%)	$\lambda_{max} \downarrow$
ViT-B/16	84.58	739
ViT-B/16 $r16 - \widehat{0}$	80.44 (-4.14)	7388 (9.9x)
ViT-B/16 $r16 - \widehat{2}$	83.40 (-1.18)	4248 (5.7x)
ViT-B/16-SAM	80.28	21
ViT-B/16-SAM $r16 - \widehat{0}$	79.32 (-0.96)	33 (1.6x)
ViT-B/16-SAM $r16 - \widehat{2}$	80.27 (-0.01)	28 (1.3x)

3.3. Local-Global Token Merging (LGTM)

In this section, we present our spatially-aware token merging module and discuss various design choices and motivations.

To Drop or to Merge. The benefit of merging over pruning can be understood through the following intuition. Off-the-shelf ViT models are commonly pretrained with a dense token distribution (no token dropping). Thus, a trained model “expects” to see not only task-relevant tokens but

Table 3. **Drop vs. Merge** comparison using ViT-L/16 with $r = 7$. Merging retains accuracy more effectively in training-free settings. X_{pre} is right before and X_{attn} is inside the attention block.

FEATURES	DROP		MERGE	
	ACC	IM/S	ACC	IM/S
RANDOM	2.96	131.3	61.89	136.5
X_{pre}	82.1	129.1	83.18	125.7
X_{attn}	81.58	129.1	83.41	125.7
K	71.86	130.7	83.51	132.1
Q	73.65	130.3	83.25	133.6
V	78.9	130.3	83.44	132.3

also less relevant ones like background tokens. Less informative tokens can also function as regularization, which makes it *risky to assume that less important tokens can be removed without degrading the prediction performance*. On the other hand, if the network is trained with importance-based token dropping, it may learn to process sharper feature distributions that contain dense task-relevant information.

Given that task-relevancy is not a robust signal for compression, token merging reformulates the problem from a *discrimination task to a retention task*. Rather than trying to discriminate task-irrelevant tokens by some heuristic (e.g., attention score from the class token, magnitude, etc.), token merging attempts to *retain* the same dense distribution of features that may also contain task-irrelevant features.

Merging Heuristic. As in Table 3, we empirically validate this intuition by comparing token dropping to token merging using various features as importance scores. For dropping, we remove r *least important tokens* with the lowest L2 norms. For merging, we merge the r *most similar tokens* by using the cosine similarity score between tokens; details of the merging process are provided in the next section.

Across various features used as importance or similarity scores, merging is advantageous when it is applied as a post-training technique. Dropping by X_{pre} gives a surprisingly good performance but lags slightly behind the merging technique. For merging, similarity scores from the K matrix yield the highest performance, which means it best summarizes the tokens even more than X_{pre} or X_{attn} that has a larger embedding size per token. This may be an effect of overparameterized embeddings, where having more channels can result in noise. Since K has less number of channels through the multi-head attention, its compact representation can resolve this problem.

Vanilla Token Merger. We describe the original ToMe (Token Merging) module (Bolya et al., 2022), which is used as a building block in our pipeline. The task of merging similar tokens can be formulated as a *Bipartite Soft Matching* prob-

lem. This is preferable to iterative clustering approaches (e.g., k -means) since it can be parallelized. The module is described below:

1. Partition the tokens into two sets \mathbb{A} and \mathbb{B} of roughly equal size;
2. Draw an edge from each token in \mathbb{A} to its most similar token in \mathbb{B} ;
3. Keep the r most similar edges;
4. Merge tokens that are still connected (e.g. weighted average); and
5. Concatenate the two sets back together.

ToMe is inserted into each transformer block between the attention and MLP modules, which can effectively reduce the number of tokens. However, in high compression regions (2x FLOP count reduction), we observe that the similarity score between merged tokens drops significantly as in Figure 3. For moderate compression rates ($r = 10$), the merged tokens have increasing similarity scores which is desirable to have similar tokens be merged. However, for higher compression rates ($r = 20$), the similarity decreases over the layers which can degrade performance.

This effectively fails to satisfy the assumption that merging similar tokens will retain accuracy. When non-similar tokens are merged, it becomes an interpolation of two distinct embeddings. This now requires the model to generalize to potentially unknown feature distributions, which can degrade performance. Given this challenge, we search for another similarity metric that can make the merging more robust to high compression regimes.

Role of Spatial Bias. A unique component of ViT compared to CNN is its positional encoding. Initialized as random embeddings associated with each token, the network learns the spatial relationships between tokens and encodes them into parameters. Intuitively, this can be understood as neighboring pixels in an image having stronger semantic relationships with each other. For example, a picture of an animal has contiguous body parts where *spatial proximity* correlates well with *semantic similarity*.

To this extent, we visualize the learned position embeddings and select four representative tokens to see which tokens they are most spatially related to. As in Figure 4, the reference token (darkest point) is most spatially similar to the quadrant that is associated with. Motivated by this fact and the success of using locality-augmented ViT architecture from the Swin Transformer (Liu et al., 2021b), we propose a local merging scheme.

Localized Merging. Instead of globally searching for similar tokens, we constrain the search space to local windows.

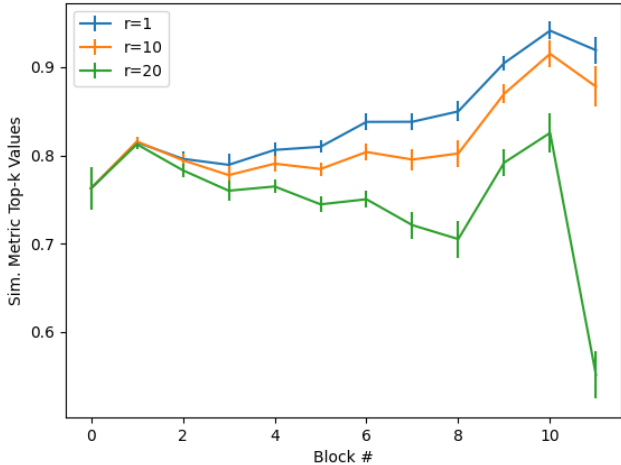


Figure 3. Accuracy Degradation for Vanilla ToMe is driven by merged tokens being less similar for large r values (high-compression). Here, the similarity score is higher the better.

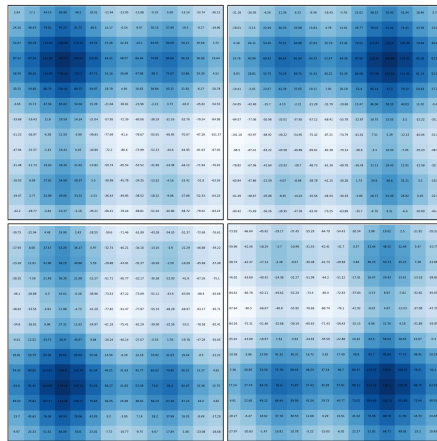


Figure 4. Learned Positional Embeddings suggest that tokens in the same quadrant are spatially related and can augment the similarity metric.

The input tokens of the grid (H,W) are partitioned into four equally-sized parts with some pre-defined window size, w . To minimize complexity, we fix $w = 7$ in all of our experiments as it nicely divides 14×14 grid of tokens (224×224 resolution divided by common patch size of 16). When the number of tokens is not divisible by w , we apply padding in the bottom and right sides of the grid fashion to retain the 2D formation.

Batched Inference. Windows can be stacked to efficiently merge tokens in parallel. This is possible because token merging is applied independently for each example in a batch, and the window dimension can be fused into the batch dimension B in the following manner: $(B, H, W) \rightarrow (B, H/w, w, W/w, w) \rightarrow (B * H/w * W/w, w, w)$.

Algorithm 1 DFE + LGTM Inference Pipeline

```

Input: skip  $s$ , window  $w$ , transition  $t$ , token reduction  $r$ 
for  $i = 0$  to  $numBlocks - 1$  do
  if  $i < s$  then
    Skip token merging
  else
    if  $i < s + t$  then
      Partition tokens into  $w \times w$  sized windows
      Merge  $\lceil r/numW \rceil$  tokens per window
      Increment  $w$ 
    else
      Globally merge  $r$  pairs
    end if
  end if
end for

```

Table 4. **Design Choices.** For our spatially augmented ViT-L/16 $r = 18$, the K embeddings yield the best tradeoff.

	RANDOM	X_{pre}	X_{attn}	K	Q	V
ACC	59.60	82.81	82.68	82.85	82.35	82.56
IM/S	589	551.8	552.2	591.5	589.2	589.5

Tracking Token Location. After tokens are merged, a single token now shares the location of multiple tokens. Following ToMe’s approach in tracking token size, the location vector containing token IDs are computed with a weighted average. Here, the weight (or token size) saves how many tokens it has already merged with. By sorting the 1D vector containing token IDs along a 2D grid of size $(2*w, 2*w)$ in each block, we approximately track the locations with some loss of information in the axis we do not sort along.

Inference Pipeline. As in Algorithm 1, our compression framework augments ToMe with DFE and LGTM. The skip value s is the number of initial layers to skip merging. The window size w is the local merging window. The transition value t is the number of times local merging is applied. Finally, the token reduction value r controls the number of tokens to merge in each layer it is applied to.

To minimize complexity, s and w are fixed according to the model architecture as discussed in Section 3.1 and Section 3.3, respectively. t can be computed offline, which is the block number where the window size is greater than the closest squared root of the patch sequence length. The only hyperparameter to tune is r which controls the accuracy-efficiency tradeoff.

Design Choices. We also ablate the best similarity heuristic for our framework. As shown in Table 4, K is the best choice, the same as the vanilla ToMe. Random selection has the worst accuracy while choosing X_{pre} and X_{attn} degrades the throughput.

Table 5. **Comparison to Prior Work.** On DeiT-S, our framework provides competitive performance even compared to works that use training. † Merging while training gives $1.5\times$ speedup.

	TOP-1	GFLOPS	EPOCHS	E2E (HRS)
DEiT-S/16	79.8	4.6	–	–
DYNAMICViT	79.3	2.9	30	44.8
A-ViT	78.6	2.9	100	76.4
E-ViT	79.1	2.6	300	154.4
ToMe	79.4	2.7	300	102.2†
ToMe	78.9	2.8	0	–
OURS-DFE	79.2	2.8	0	–
OURS-FULL	78.6	2.5	0	–

4. Experiments

4.1. Setup

Dataset and Models. We conduct our experiments in the ImageNet-1K dataset (Russakovsky et al., 2015) to evaluate the effectiveness of our method in accelerating classification tasks off the shelf. Both DeiT (Touvron et al., 2021) and ViT models trained with AugReg (Steiner et al., 2021) are used to test the generalizability of our method across different backbones and training methods.

Metrics. The computational cost is measured in FLOPS with the TorchProfiler library. Inference throughput is measured on an Nvidia RTX A6000 GPU with a fixed batch size of 32 averaged over 50 runs. End to End (E2E) training time is measured in a single 8 GPU node; we evaluate the training time of one epoch and multiply it by the total number of epochs to obtain the final time.

4.2. Acceleration with Training

As in Table 5, our framework can achieve comparable accuracy and GFLOPS while being *two orders of magnitude faster* than existing approaches thanks to zero training. For example, E-ViT (Liang et al., 2022) takes around 154 single GPU hours for one run. Since it requires running the method for each target speedup, the cost of deploying to various resource constraints can become quickly intractable.

4.3. Acceleration without Training

4.3.1. ViT MODEL SWEEPS

In Figure 5, we apply our framework to ViT-S, ViT-B, and ViT-L *off-the-shelf* with 224px and patch size 16. For each model, we try three configurations: 1) ToMe, 2) DFE only, and 3) Full (DFE + LGTM). We vary r to construct two Pareto curves that compare Top-1 accuracy to #MACs and throughput. Note that we sweep with higher r values with the DFE and Full configuration to match the computational load of vanilla ToMe.

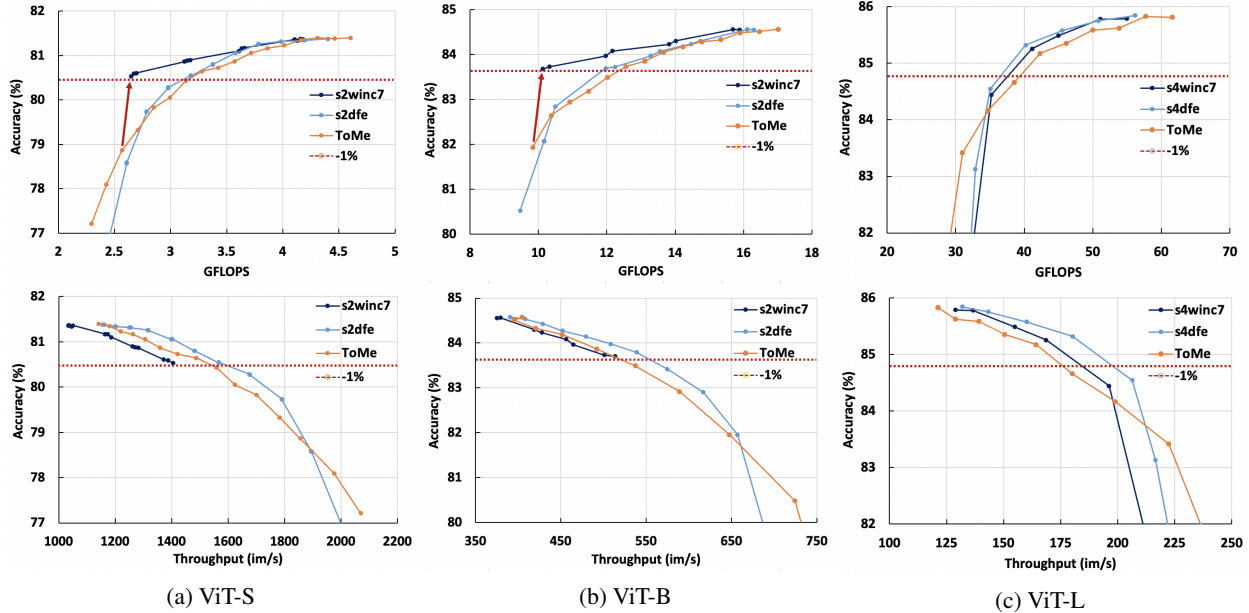


Figure 5. **Model Sweep.** We apply our inference pipeline to several state-of-the-art ViT models in a *training-free* fashion. DFE and LGTM configs are fixed by the network architecture, only varying parameter r to produce Top-1 Acc. vs. GFLOPS curves on ImageNet-1k.

Floating Point Operations. We can see that our framework consistently gives better results than ToMe when constraining the accuracy degradation to 1%, which is a standard measure for a tolerable loss. Remarkably, we can save 45% and 42% of the FLOPS within 1% loss for ViT-S and ViT-B, respectively. Yet, the success of LGTM inversely scales with model size, showing a negligible gain for ViT-L.

Throughput. In contrast to the success of LGTM in saving FLOPS, we observe that a plain DFE consistently outperforms other configurations in accelerating throughput. We think this is because the additional data movements, such as sorting, padding, and modifying tensor dimensions, cause a nontrivial overhead. Interestingly, this overhead is less obvious for larger models, as the LGTM curve shifts to the right, eventually surpassing ToMe in ViT-L by a close margin.

4.4. Sharpness-aware Model

To show the robustness of SAM models to compression, we use ViT-B-SAM/16 and evaluate ToMe and DFE settings. We present below the results as shown in Figure 6 and Figure 8.

Vanilla ToMe. With the vanilla ToMe alone, the model trained with SAM achieves $1.77\times$ speedup and saves 50% FLOPS with 1% loss. Compared to its counterpart pre-trained with the Adam optimizer, the model pre-trained with SAM improves the accuracy loss by 3% at $r = 16$.

Dense Extractor. The robustness of models pre-trained with SAM is further pronounced when combined with the DFE

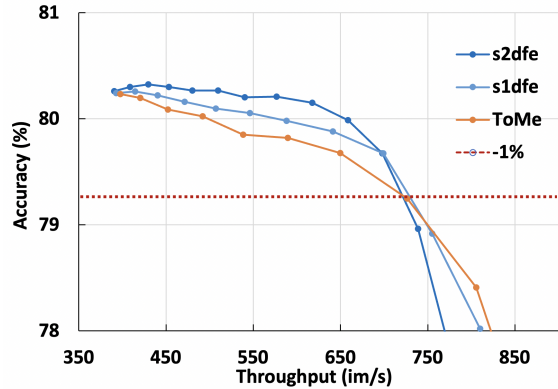


Figure 6. SAM helps ViT-B to retain negligible accuracy loss for higher throughputs. DFE can further boost this effect with layer skipping.

configuration. Remarkably, $s = 2$ achieves $1.6\times$ speedup with 44% FLOPS savings with a mere **0.2%** loss. When the compression is taken to the extreme, the Pareto curves eventually follow a sharp decline, similar to the normal ViTs.

4.5. Analysis

In this section, we introduce analysis to validate the efficacy of our design choices.

Skipping with DFE. How many blocks should we initially skip for the plain DFE setting to best optimize the throughput? According to Table 6, $s = 4$ yields the best accuracy-speedup tradeoff. This validates our choice to skip the first

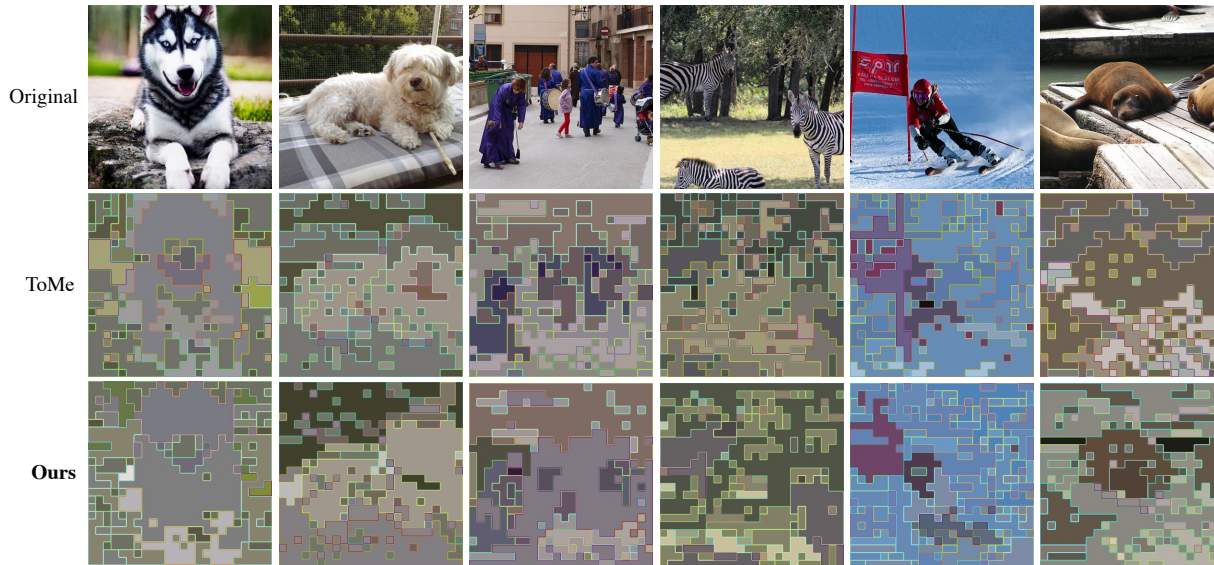


Figure 7. **Image Visualizations.** Qualitative comparison of LGTM using an off-the-shelf ViT-L₃₈₄ model. Compared to vanilla ToMe (Bolya et al., 2022), LGTM merges more contiguous patches that are semantically similar. Caveat: 384 resolution was chosen for visualization purposes, as its finer granularity helps highlight the effect of merging; the performance gain here is statistically trivial.

Table 6. Ablating skip value for DFE on ViT-L.

SKIP VALUE	ACC. LOSS (%)	SPEEDUP	#MACS (G)
0	1.58	1.58×	34.7
2	1.37	1.56×	35.2
4	1.27	1.61×	35.0

Table 7. Ablating skip value for DFE + LGTM on ViT-S.

SKIP VALUE	ACC. LOSS (%)	SPEEDUP	#MACS (G)
0	0.96	1.25×	3.14
1	0.86	1.06×	2.85
2	0.86	1.13×	2.65

one-sixth of the network since ViT-L has a depth of 24.

Skipping with LGTM. We know LGTM best optimizes for computation on smaller model sizes. As in Table 7, $s = 2$ yields the best accuracy-computation tradeoff for ViT-S with a depth of 12. This validates that skipping the first one-sixth of the network is still optimal in the context of LGTM.

4.6. Visualizations

In Figure 7, we show the input tokens belonging to the final merged token. We use $r = 24$ for ToMe and $r = 28$ with $s = 4$ and $w = 8$ for our framework. Note that the parameters are different since the resolution is higher. To match the final token count, we do not merge the last block in our framework.

We see that in the second image, the face of the Maltese is

contiguously merged into a single token for us, while ToMe separates out the nose. The same is true for the body of a Huskey in the first photo and the people in the center of the third photo, where our framework tends to merge more contiguous tokens.

Moreover, our framework is able to localize important features when necessary as illustrated in the fifth photo. For ToMe, the legs of a skier are merged with the background snow while we can localize the legs from the snow. Similarly, the sixth photo shows that our framework localizes the head of the center sea lion while ToMe does not.

5. Conclusion and Future Work

In this work, we proposed a fast training-free compression framework for Vision Transformers. We found that the divergence of token features in the first few blocks may negatively impact merging, thus introducing the Dense Feature Extractor. We further augment the similarity metric with spatial bias via local merging. Combining these methods, we advance the SotA training-free ViT compression by $1.34\times$ in throughput and $1.18\times$ in MACs. We hope to inspire additional lines of research in making large transformer models more accessible and sustainable in practice.

Limitations. We observe that our inference pipeline does not fully optimize for both GFLOPS and Throughput in a single configuration. In the future, we hope to further optimize the code for the LGTM method to realize the observed MAC savings into throughput speedup.

References

- Beyer, L., Zhai, X., Royer, A., Markeeva, L., Anil, R., and Kolesnikov, A. Knowledge distillation: A good teacher is patient and consistent. In *Proceedings of the IEEE/CVF Conference on Computer Vision and Pattern Recognition*, pp. 10925–10934, 2022.
- Bolya, D., Fu, C.-Y., Dai, X., Zhang, P., Feichtenhofer, C., and Hoffman, J. Token merging: Your vit but faster. *arXiv preprint arXiv:2210.09461*, 2022.
- Chen, B., Dao, T., Liang, K., Yang, J., Song, Z., Rudra, A., and Re, C. Pixelated butterfly: Simple and efficient sparse training for neural network models. *arXiv preprint arXiv:2112.00029*, 2021.
- Chen, X., Hsieh, C., and Gong, B. When vision transformers outperform resnets without pre-training or strong data augmentations. In *The Tenth International Conference on Learning Representations, ICLR 2022, Virtual Event, April 25-29, 2022*. OpenReview.net, 2022. URL <https://openreview.net/forum?id=LtKcMgGOeIt>.
- Devlin, J. et al. BERT: pre-training of deep bidirectional transformers for language understanding. In *Conference of the North American Chapter of the Association for Computational Linguistics: Human Language Technologies*. Association for Computational Linguistics, 2019.
- Dosovitskiy, A., Beyer, L., Kolesnikov, A., Weissenborn, D., Zhai, X., Unterthiner, T., Dehghani, M., Minderer, M., Heigold, G., Gelly, S., et al. An image is worth 16x16 words: Transformers for image recognition at scale. *arXiv preprint arXiv:2010.11929*, 2020.
- Foret, P., Kleiner, A., Mobahi, H., and Neyshabur, B. Sharpness-aware minimization for efficiently improving generalization. In *9th International Conference on Learning Representations, ICLR 2021, Virtual Event, Austria, May 3-7, 2021*. OpenReview.net, 2021. URL <https://openreview.net/forum?id=6Tm1mposlrM>.
- Han, S., Mao, H., and Dally, W. J. Deep compression: Compressing deep neural networks with pruning, trained quantization and Huffman coding. *arXiv preprint arXiv:1510.00149*, 2015.
- Hinton, G. E., Vinyals, O., and Dean, J. Distilling the knowledge in a neural network. *CoRR*, abs/1503.02531, 2015.
- Kim, S., Gholami, A., Yao, Z., Mahoney, M. W., and Keutzer, K. I-BERT: integer-only BERT quantization. In Meila, M. and Zhang, T. (eds.), *Proceedings of the 38th International Conference on Machine Learning, ICML 2021, 18-24 July 2021, Virtual Event*, volume 139 of *Proceedings of Machine Learning Research*, pp. 5506–5518. PMLR, 2021. URL <http://proceedings.mlr.press/v139/kim21d.html>.
- Kingma, D. P. and Ba, J. Adam: A method for stochastic optimization. *arXiv preprint arXiv:1412.6980*, 2014.
- Kong, Z., Dong, P., Ma, X., Meng, X., Niu, W., Sun, M., Shen, X., Yuan, G., Ren, B., Tang, H., Qin, M., and Wang, Y. Spvit: Enabling faster vision transformers via latency-aware soft token pruning. In Avidan, S., Brostow, G., Cissé, M., Farinella, G. M., and Hassner, T. (eds.), *Computer Vision – ECCV 2022*, pp. 620–640, Cham, 2022. Springer Nature Switzerland.
- Kurtic, E., Campos, D., Nguyen, T., Frantar, E., Kurtz, M., Fineran, B., Goin, M., and Alistarh, D. The optimal BERT surgeon: Scalable and accurate second-order pruning for large language models. *CoRR*, abs/2203.07259, 2022. doi: 10.48550/arXiv.2203.07259. URL <https://doi.org/10.48550/arXiv.2203.07259>.
- Kwon, W., Kim, S., Mahoney, M. W., Hassoun, J., Keutzer, K., and Gholami, A. A fast post-training pruning framework for transformers. *arXiv preprint arXiv:2204.09656*, 2022.
- Liang, Y., Ge, C., Tong, Z., Song, Y., Wang, J., and Xie, P. Evit: Expediting vision transformers via token reorganizations. In *The Tenth International Conference on Learning Representations, ICLR 2022, Virtual Event, April 25-29, 2022*. OpenReview.net, 2022. URL https://openreview.net/forum?id=BjyvwnXXVn_.
- Liu, Z., Lin, Y., Cao, Y., Hu, H., Wei, Y., Zhang, Z., Lin, S., and Guo, B. Swin transformer: Hierarchical vision transformer using shifted windows. In *2021 IEEE/CVF International Conference on Computer Vision, ICCV 2021, Montreal, QC, Canada, October 10-17, 2021*, pp. 9992–10002. IEEE, 2021a. doi: 10.1109/ICCV48922.2021.00986. URL <https://doi.org/10.1109/ICCV48922.2021.00986>.
- Liu, Z., Lin, Y., Cao, Y., Hu, H., Wei, Y., Zhang, Z., Lin, S., and Guo, B. Swin transformer: Hierarchical vision transformer using shifted windows. In *Proceedings of the IEEE/CVF International Conference on Computer Vision*, pp. 10012–10022, 2021b.
- Marin, D., Chang, J. R., Ranjan, A., Prabhu, A., Rastegari, M., and Tuzel, O. Token pooling in vision transformers. *CoRR*, abs/2110.03860, 2021. URL <https://arxiv.org/abs/2110.03860>.
- Mundhenk, T. N., Chen, B. Y., and Friedland, G. Efficient saliency maps for explainable ai. *arXiv preprint arXiv:1911.11293*, 2019.

- Na, C., Mehta, S. V., and Strubell, E. Train flat, then compress: Sharpness-aware minimization learns more compressible models. *arXiv preprint arXiv:2205.12694*, 2022.
- Rao, Y., Zhao, W., Liu, B., Lu, J., Zhou, J., and Hsieh, C. Dynamicvit: Efficient vision transformers with dynamic token sparsification. In Ranzato, M., Beygelzimer, A., Dauphin, Y. N., Liang, P., and Vaughan, J. W. (eds.), *Advances in Neural Information Processing Systems 34: Annual Conference on Neural Information Processing Systems 2021, NeurIPS 2021, December 6-14, 2021, virtual*, pp. 13937–13949, 2021. URL <https://proceedings.neurips.cc/paper/2021/hash/747d3443e319a22747fbb873e8b2f9f2-Abstract.html>.
- Russakovsky, O., Deng, J., Su, H., Krause, J., Satheesh, S., Ma, S., Huang, Z., Karpathy, A., Khosla, A., Bernstein, M., et al. Imagenet large scale visual recognition challenge. *International journal of computer vision*, 115: 211–252, 2015.
- Ryoo, M. S., Piergiovanni, A. J., Arnab, A., Deghani, M., and Angelova, A. Tokenlearner: Adaptive space-time tokenization for videos. In Ranzato, M., Beygelzimer, A., Dauphin, Y. N., Liang, P., and Vaughan, J. W. (eds.), *Advances in Neural Information Processing Systems 34: Annual Conference on Neural Information Processing Systems 2021, NeurIPS 2021, December 6-14, 2021, virtual*, pp. 12786–12797, 2021. URL <https://proceedings.neurips.cc/paper/2021/hash/6a30e32e56fce5cf381895dfe6ca7b6f-Abstract.html>.
- Shen, S., Dong, Z., Ye, J., Ma, L., Yao, Z., Gholami, A., Mahoney, M. W., and Keutzer, K. Q-BERT: hessian based ultra low precision quantization of BERT. In *The Thirty-Fourth AAAI Conference on Artificial Intelligence, AAAI 2020, The Thirty-Second Innovative Applications of Artificial Intelligence Conference, IAAI 2020, The Tenth AAAI Symposium on Educational Advances in Artificial Intelligence, EAAI 2020, New York, NY, USA, February 7-12, 2020*, pp. 8815–8821. AAAI Press, 2020. URL <https://ojs.aaai.org/index.php/AAAI/article/view/6409>.
- Steiner, A., Kolesnikov, A., Zhai, X., Wightman, R., Uszkoreit, J., and Beyer, L. How to train your vit? data, augmentation, and regularization in vision transformers. *CoRR*, abs/2106.10270, 2021. URL <https://arxiv.org/abs/2106.10270>.
- Tian, Z., Yi, J., Bai, Y., Tao, J., Zhang, S., and Wen, Z. Synchronous transformers for end-to-end speech recognition. In *2020 IEEE International Conference on Acoustics, Speech and Signal Processing, ICASSP 2020, Barcelona, Spain, May 4-8, 2020*, pp. 7884–7888. IEEE, 2020. doi: 10.1109/ICASSP40776.2020.9054260. URL <https://doi.org/10.1109/ICASSP40776.2020.9054260>.
- Touvron, H., Cord, M., Douze, M., Massa, F., Sablayrolles, A., and Jégou, H. Training data-efficient image transformers and distillation through attention. In Meila, M. and Zhang, T. (eds.), *Proceedings of the 38th International Conference on Machine Learning, ICML 2021, 18-24 July 2021, Virtual Event, volume 139 of Proceedings of Machine Learning Research*, pp. 10347–10357. PMLR, 2021. URL <http://proceedings.mlr.press/v139/touvron21a.html>.
- Vaswani, A., Shazeer, N., Parmar, N., Uszkoreit, J., Jones, L., Gomez, A. N., Kaiser, Ł., and Polosukhin, I. Attention is all you need. *Advances in neural information processing systems*, 30, 2017.
- Voita, E., Talbot, D., Moiseev, F., Sennrich, R., and Titov, I. Analyzing multi-head self-attention: Specialized heads do the heavy lifting, the rest can be pruned. In Korhonen, A., Traum, D. R., and Màrquez, L. (eds.), *Proceedings of the 57th Conference of the Association for Computational Linguistics, ACL 2019, Florence, Italy, July 28- August 2, 2019, Volume 1: Long Papers*, pp. 5797–5808. Association for Computational Linguistics, 2019. doi: 10.18653/v1/p19-1580. URL <https://doi.org/10.18653/v1/p19-1580>.
- Wortsman, M., Ilharco, G., Gadre, S. Y., Roelofs, R., Gontijo-Lopes, R., Morcos, A. S., Namkoong, H., Farhadi, A., Carmon, Y., Kornblith, S., and Schmidt, L. Model soups: averaging weights of multiple finetuned models improves accuracy without increasing inference time. In Chaudhuri, K., Jegelka, S., Song, L., Szepesvari, C., Niu, G., and Sabato, S. (eds.), *Proceedings of the 39th International Conference on Machine Learning*, volume 162 of *Proceedings of Machine Learning Research*, pp. 23965–23998. PMLR, 17–23 Jul 2022. URL <https://proceedings.mlr.press/v162/wortsman22a.html>.
- Xiao, G., Lin, J., Seznec, M., Demouth, J., and Han, S. Smoothquant: Accurate and efficient post-training quantization for large language models. *arXiv preprint arXiv:2211.10438*, 2022.
- Yin, H., Vahdat, A., Alvarez, J. M., Mallya, A., Kautz, J., and Molchanov, P. A-vit: Adaptive tokens for efficient vision transformer. In *IEEE/CVF Conference on Computer Vision and Pattern Recognition, CVPR 2022, New Orleans, LA, USA, June 18-24, 2022*, pp. 10799–10808.

IEEE, 2022. doi: 10.1109/CVPR52688.2022.01054.
URL <https://doi.org/10.1109/CVPR52688.2022.01054>.

Zhang, Q., Zuo, S., Liang, C., Bukharin, A., He, P., Chen, W., and Zhao, T. Platon: Pruning large transformer models with upper confidence bound of weight importance. In *International Conference on Machine Learning*, pp. 26809–26823. PMLR, 2022.

A. Additional Results.

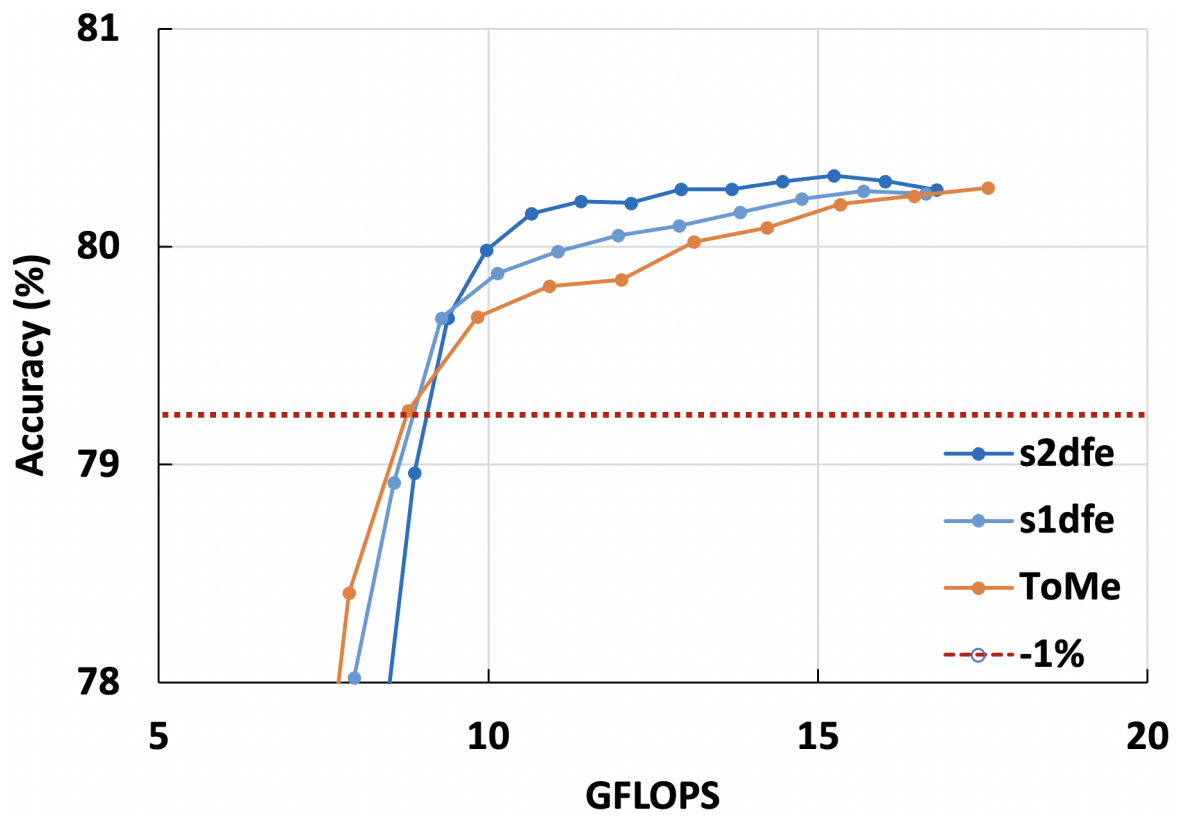


Figure 8. GFLOPS pareto curve for ViT-B-SAM/16 model.

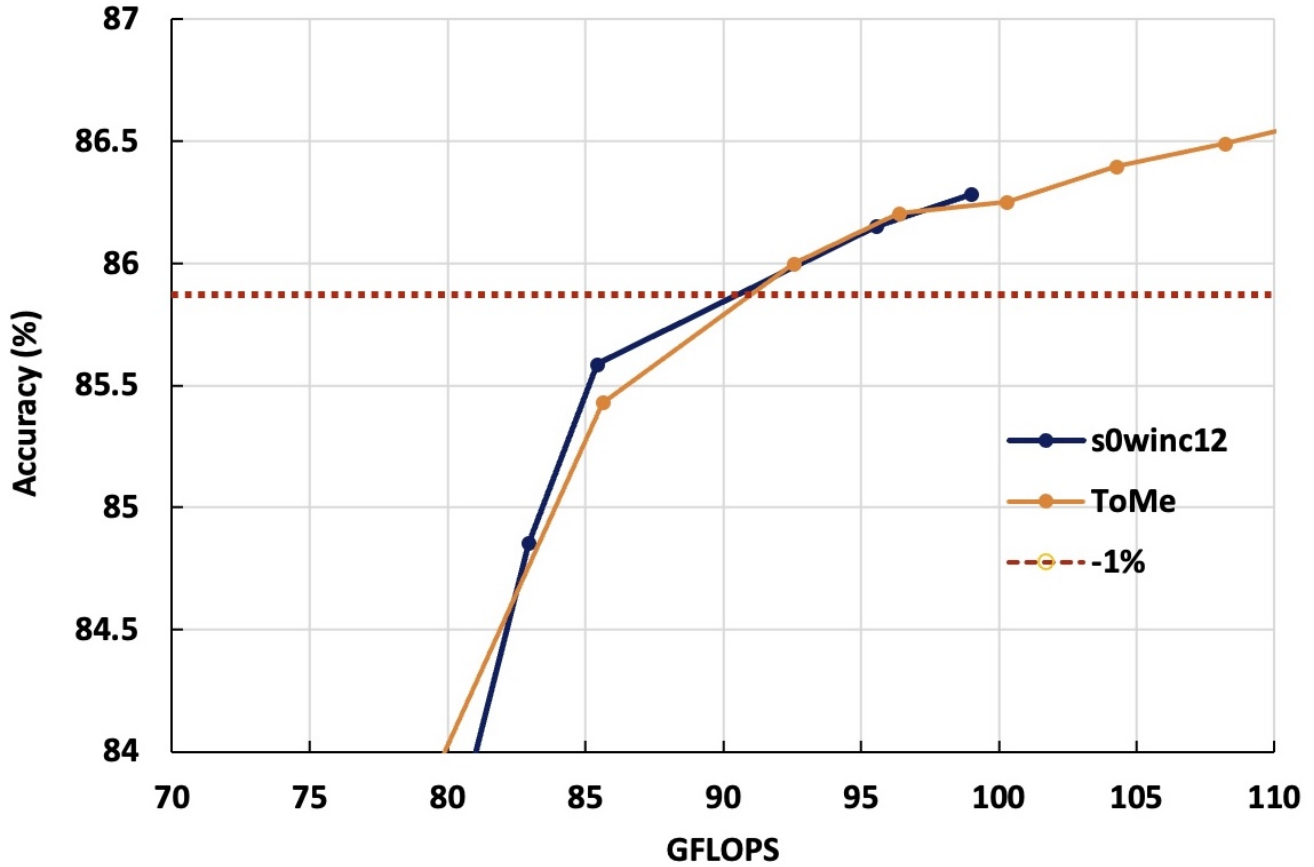


Figure 9. GFLOPS pareto curve for ViT-L-384 model.

Table 8. Ablating DFE and LGTM on DeiT-S/16.

ToMe		w/ DFE		w/ DFE + LGTM	
Top1	GFlops	Top1	GFlops	Top1	GFlops
79.51	3.6	79.69	3.6	79.61	3.6
79.29	3.1	79.55	3.2	79.38	3.3
78.96	2.8	79.53	2.9	79.42	3.0
78.32	2.5	78.25	2.5	78.61	2.5
78.03	2.3	77.48	2.3	78.33	2.4